Roles of Small Laccases from Streptomyces in Lignin Degradation

ARTICLE *in* BIOCHEMISTRY · MAY 2014

Impact Factor: 3.02 · DOI: 10.1021/bi500285t · Source: PubMed

7 AUTHORS, INCLUDING:

Tiit Lukk
Cornell University
13 PUBLICATIONS **152** CITATIONS
SEE PROFILE

Jose Solbiati
University of Illinois, Urbana-Champaign
15 PUBLICATIONS **588** CITATIONS
SEE PROFILE

Stefan Bauer
University of California, Berkeley
42 PUBLICATIONS **1,414** CITATIONS
SEE PROFILE

John Cronan
University of Illinois, Urbana-Champaign
367 PUBLICATIONS **15,502** CITATIONS
SEE PROFILE

BIOCHEMISTRY
including biophysical chemistry & molecular biology

Article

pubs.acs.org/biochemistry

Roles of Small Laccases from *Streptomyces* in Lignin Degradation

Sudipta Majumdar,*[,†,§] Tiit Lukk,[†,∥] Jose O. Solbiati,[†] Stefan Bauer,[‡] Satish K. Nair,[†] John E. Cronan,[†] and John A. Gerlt[†]

[†]Institute for Genomic Biology, University of Illinois at Urbana-Champaign, Urbana, Illinois 61801, United States

[‡]Energy Biosciences Institute, University of California, Berkeley, California 94720, United States

Supporting Information

ABSTRACT: Laccases (EC 1.10.3.2) are multicopper oxidases that can oxidize a range of substrates, including phenols, aromatic amines, and nonphenolic substrates. To investigate the involvement of the small *Streptomyces* laccases in lignin degradation, we generated acid-precipitable polymeric lignin obtained in the presence of wild-type *Streptomyces coelicolor* A3(2) (SCWT) and its laccase-less mutant (SCΔLAC) in the presence of *Miscanthus x giganteus* lignocellulose. The results showed that strain SCΔLAC was inefficient in degrading lignin compared to strain SCWT, thereby supporting the importance of laccase for lignin degradation by *S. coelicolor* A3(2). We also studied the lignin degradation activity of laccases from *S. coelicolor* A3(2), *Streptomyces lividans* TK24, *Streptomyces viridosporus* T7A, and *Amycolatopsis* sp. 75iv2 using both lignin model compounds and ethanosolv lignin. All four laccases degraded a phenolic model compound (LM-OH) but were able to oxidize a nonphenolic model compound only in the presence of redox mediators. Their activities are highest at pH 8.0 with a low k_{rel}/K_{app} for LM-OH, suggesting that the enzymes' natural substrates must be different in shape or chemical nature. Crystal structures of the laccases from *S. viridosporus* T7A (SVLAC) and *Amycolatopsis* sp. 75iv2 were determined both with and without bound substrate. This is the first report of a crystal structure for any laccase bound to a nonphenolic *β*-O-4 lignin model compound. An additional zinc metal binding site in SVLAC was also identified. The ability to oxidize and/or rearrange ethanosolv lignin provides further evidence of the utility of laccase activity for lignin degradation and/or modification.

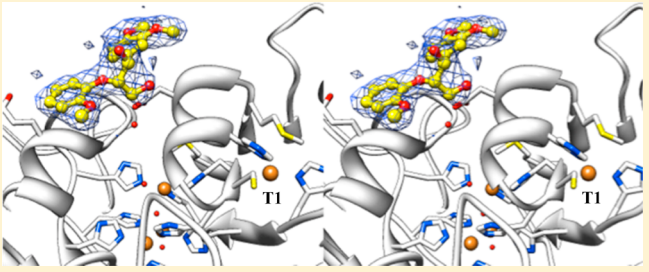

Lignocellulosic biomass, composed of lignin, cellulose, and hemicellulose, has been targeted as a potential source of renewable bioenergy. Lignin accounts for 20% of lignocellulosic material and is an integral part of all higher plants and the second most abundant organic polymer in nature after cellulose. Lignin serves as a key structural component and an outer protective shield against biochemical hydrolysis of the energy rich and more easily metabolizable cellulose and hemicellulose.[1,2] Therefore, lignin removal is required for efficient utilization of lignocellulosic biomass for the production of biofuels and other cellulose-based chemicals. Lignin has a complex, heterogeneous, polymeric structure derived from oxidative coupling of three phenylpropanoid monomers, *p*-coumaryl, coniferyl, and sinapyl alcohols (Figure S1 of the Supporting Information).[3] The complexity of the lignin structure and its covalent connectivity to hemicellulose provide not only mechanical and structural stability but also resistance to chemical and biological degradation. Most of the available chemical pretreatment methods for lignin degradation have adverse effects on the later stages of energy conversion from cellulosic biomass and generate toxic waste products.[4−6] For more ecologically favorable applications, methods using lignin-degrading microbes and/or their enzymes may provide a more efficient and environmentally sound approach for accessing renewable lignocellulosic biomass.

A variety of microorganisms, including certain fungi and bacteria, can degrade lignin, thus allowing access to plant carbohydrates as a rich energy source.[7−10] Among these microorganisms, white-rot fungi have attracted widespread attention because of their powerful lignin-degrading enzymatic systems.[11,12] However, utilization of these enzymes is problematic because of their poor stability in industrial processes, as well as the difficulty in developing efficient heterologous systems for enzyme expression and purification. Consequently, much attention has been paid to lignin degradation by bacterial species.[13−15] The most extensively studied are actinomycetes, particularly *Streptomyces* species because of their reported efficiency in lignin degradation, established genetic and molecular engineering tools, and the availability of complete genome sequences.[16,17] In spite of this, very little is known about either the involvement of specific enzymes or the molecular mechanism of lignin degradation. Extensive work has been performed with *Streptomyces viridosporus* T7A in which an extracellular lignin peroxidase (LiP) was reported to possess significant lignin degradation activity.[18−20] Despite some reports in the literature, bona fide extracellular lignin-degrading

Received: March 7, 2014
Revised: May 27, 2014
Published: May 28, 2014

peroxidases have yet to be identified in *S. viridosporus* T7A.[9,18,19,21,22] Recently, an extracellular DyP peroxidase from *Amycolatopsis* sp. 75iv2 was characterized and reported to be a lignin-degrading enzyme.[14,23] Efforts to find enzymes responsible for lignin degradation by *Streptomyces* resulted in our discovery of a small laccase, a copper-dependent phenol oxidase.[24]

Laccases (*p*-diphenol:dioxygen oxidoreductase) are copper-containing enzymes that can oxidize a range of aromatic and nonaromatic compounds containing hydroxyl and amine groups in the presence of atmospheric oxygen.[25,26] These enzymes are produced not only by eukaryotes such as fungi and plants but also by prokaryotes, including a wide range of Gram-positive and Gram-negative bacteria.[25,27,28] Although laccases are believed to be involved in lignin synthesis in plants and in cell pigment formation, as well as metal oxidation in fungi and bacteria, their physiological roles are unclear. The most detailed biochemical characterization of laccases was conducted with the enzymes from the basidomycetes, *Pycnoporus cinnabarinus* and *Trametes versicolor*, wherein laccases were shown to play important roles in lignin degradation.[29,30] Recently, laccases from actinomycetes were reported to have *in vitro* activity against a wide range of substrates. These enzymes were designated as "small laccases" because of their sequence similarity but smaller size compared to fungal laccases.[24] Small laccases have been extensively exploited in the pulp and paper industries for dye decolorization and biobleaching because of their high oxidizing power, pH versatility, and thermal stability.[24,31] Despite the advantages bacterial enzymes may offer versus fungal enzymes, no detailed biochemical studies have been conducted using either native lignocellulosic biomass or lignin model compounds as substrates. Improved knowledge of bacterial laccases and their role in lignin degradation will have a significant impact on a wide array of biotechnologies focused on lignin degradation.

The purpose of this work is to investigate the importance of the small laccases from *Streptomyces* in both *in vivo* and *in vitro* lignin degradation activity assays using lignocellulosic biomass from *Miscanthus x giganteus*, ethanosolv lignin, and *β*-O-4 lignin model compounds.[3,32] An *S. coelicolor* A3(2) laccase deficient mutant (SCΔLAC) was constructed to assess its *in vivo* lignin degradation activity. Using ethanosolv lignin and *β*-O-4 lignin model compounds, we characterized four different small laccases from *S. coelicolor* A3(2) (SCLAC), *S. lividans* TK24 (SLLAC), *S. viridosporus* T7A (SVLAC), and *Amycolatopsis* sp. 75iv2 (AMLAC) (previously known as *Streptomyces setonii* and *Streptomyces griseus* 75iv2) for their *in vitro* lignin degradation/oxidation activity. For better solubility, ethanosolv lignocellulose was used as the substrate for HPLC assays.[3] Two different *β*-O-4 lignin model compounds, with and without a phenolic group (Figure S2 of the Supporting Information), were also used as substrates for spectrophotometric assays. X-ray crystal structures of small laccases, with and without a substrate bound, from *S. viridosporus* T7A and *Amycolatopsis* sp. 75iv2 are also reported.

■ MATERIALS AND METHODS

All reagents and chemicals used as buffers and substrates of the highest grade commercially available were purchased from Sigma-Aldrich, Alfa Aesar, Acros, MP Biomedicals, or Fisher. The lignin model compounds 1-(3,4-dimethoxyphenyl)-2-(2-methoxyphenoxy)-1,3-dihydroxypropane [LM-OMe (Figure S2 of the Supporting Information)] and 1-(3-methoxy-4-hydroxy)-2-(2-methoxyphenoxy)-1,3-dihydroxypropane [LM-OH (Figure S2 of the Supporting Information)] were purchased from AstaTech and used as received. The ethanosolv lignin was prepared as described previously.[32] The *T. versicolor* fungal laccase was purchased from Sigma-Aldrich. Enzymes for gene cloning were purchased from New England Biolabs. The buffers were made by mixing 0.1 M acetic acid, 0.1 M sodium acetate, 0.1 M potassium phosphate monobasic, 0.1 M potassium phosphate dibasic, 0.1 M sodium carbonate, and 0.1 M sodium bicarbonate to the desired pH. UV−vis spectrophotometric data were collected using a Cary 300 Bio Spectrophotometer. HPLC data were collected using a Beckman Coulter System Gold Spectrophotometer. Mass spectrometry data were collected using a Shimadzu LCMS-IT-TOF instrument. Protein purifications were conducted using the AKTAxpress (GE) protein purification system. X-ray diffraction data were collected at Argonne National Laboratory (Argonne, IL).

Microorganisms. Strains of *S. coelicolor* A3(2) and *S. lividans* TK24 were kindly supplied by W. W. Metcalf (University of Illinois at Urbana-Champaign), and strains of *S. viridosporus* T7A (ATCC 39115) and *Amycolatopsis* sp. 75iv2 (ATCC 39116) were obtained from American Type Culture Collection (Rockville, MD). All strains were grown in Difco ISP Medium 1, and genomic DNAs were isolated using the Wizard Genomic DNA Purification Kit (Promega) following the manufacturer's protocol.

Double Crossover In-Frame Deletion of SCO6712 by PCR Targeting. The deletion of the gene encoding the *S. coelicolor* A3(2) small laccase (SCO6712) was performed following the procedures described in the REDIRECT manual.[33] The gene was replaced with an apramycin resistance cassette, *apr*, using the PCR-targeted double crossover in-frame deletion technique.[34] The extended resistance cassette including the *apr* resistance marker, *aac(3)IV*, was amplified from pIJ773 by PCR using SCO6712-KO-F and SCO6712-KO-R primers (Table S1 of the Supporting Information). Cosmid St4C6 containing the SCO6712 gene was introduced into *Escherichia coli* BW25113/pIJ790 (*λ* RED recombination plasmid) by electroporation, and the resulting transformants were then electroporated with the extended resistance cassette to target the SCO6712 gene. The resulting mutant cosmid, St4C6ΔSCO6712::apr, was transformed into *E. coli* ET12567/pUZ8002 (nonmethylating strain) and then transferred into wild-type *S. coelicolor* A3(2) (SCWT), yielding the desired SCΔLAC mutant. The mutant was selected by virtue of its apramycin resistance and kanamycin sensitivity. The disruption of SCO6712 by the *apr* cassette was confirmed by PCR on the isolated genomic DNAs of both the SCΔLAC and SCWT using primers KO-CK-F and KO-CK-R (Table S1 of the Supporting Information). The mutation also was confirmed by DNA sequencing of PCR products.

Lignocellulose Preparation. *Miscanthus x giganteus* from an experimental field at the University of Illinois at Urbana-Champaign was used as the source of lignocellulose. The ground lignocellulose was prepared by passage of air-dried lignocellulose through an 80 *μ*m sieve (SR 300 rotor beater mill, Retsch). Dry lignocellulose (3.5 g) was placed in a 1 L Erlenmeyer flask with several glass beads and autoclaved for 1 h uncovered and then for an additional 30 min covered with aluminum foil.

Inoculum Preparation. Spores of the SCWT or SCΔLAC strain (100 *μ*L stock) were added to 200 mL of autoclaved Difco ISP Medium 1 and incubated aerobically at 30 °C for 3

days by being shaken at 220 rpm with glass beads, at which time the cells had entered into late logarithmic growth phase.[35] The cells were collected by centrifugation, washed, and resuspended in 30 mL of yeast extract mineral salt (YEMS) medium.[35]

Production of Acid-Precipitable Polymeric Lignin (APPL) from Lignocellulose. Autoclaved YEMS medium (1 L) was added to the sterile lignocellulose described previously, and 10 mL of a diluted log phase cell suspension of *Streptomyces* was added; the mixture was incubated in a 2 L flask at 30 °C for 1 week while being shaken at 220 rpm. Control reactions with YEMS medium only, YEMS medium with autoclaved lignocellulose, YEMS medium with the SCWT lacking lignocellulose, and YEMS medium with the SCΔLAC strain lacking lignocellulose were performed under similar conditions. All reactions were performed in triplicate. After 7 days, the residual lignocellulose and bacterial cells were removed by centrifugation. The supernatants then were acidified at 4 °C to pH 5.0 with concentrated HCl. The precipitated APPL was collected by centrifugation, air-dried, weighed, and analyzed chemically.

Chemical Characterization of APPL. The APPL (from SCWT or SCΔLAC) was incubated at room temperature with 0.5 mL of 72% (w/w) sulfuric acid in a modified Hungate vial capped with a rubber stopper; the mixture was vortexed every 15 min. After incubation for 1 h, 14 mL of deionized water was added and the mixture was autoclaved for 60 min. A sugar recovery standard containing the same sulfuric acid concentration was prepared in a similar way and co-autoclaved with the samples. The mixture was kept in a refrigerator overnight, and 2 mL of the clear supernatant was filtered (0.45 μm, PES) and used for HPLC analysis.

The precipitated solids were resuspended by being vortexed, and the suspension was filtered through a glass micro filter. Both the vial and filter were extensively rinsed with deionized water and dried at 105 °C overnight; the weight was determined after the sample had cooled in a desiccator for 30 min. The filter and solids were then incubated at 575 °C (ramp of 105 °C for 10 min, 200 °C for 10 min, 300 °C for 30 min, and 575 °C for 3 h and cooling to 105 °C); the weight was determined after the sample had been cooled in a desiccator for 30 min.

$$[\text{Klason lignin }\%] = [m(\text{filter} + \text{dried solid}) - m(\text{filter} + \text{ash})]/m(\text{dried initial APPL}) \times 100\%$$

For ash determination, the APPL (SCWT or SCΔLAC) was incubated on a preweighed and conditioned aluminum pan at 575 °C (ramp of 105 °C for 10 min, 200 °C for 10 min, 300 °C for 30 min, and 575 °C for 3 h and cooling to 105 °C); the weight was determined after the sample had been cooled in a desiccator for 30 min.

$$[\text{ash }\%] = [m(\text{pan} + \text{ash}) - m(\text{pan})]/m(\text{dried initial APPL}) \times 100\%$$

For HPLC, samples were analyzed at 50 °C on an HPX-87H (300 mm × 7.8 mm, Bio-Rad) column on an Agilent 1200 series liquid chromatography instrument equipped with a refractive index detector. Elution was performed with 0.005 M sulfuric acid at a flow rate of 0.6 mL/min.

Cloning, Expression, and Purification of Small Laccases from *S. coelicolor* (SCLAC), *S. lividans* (SLLAC), *S. viridosporus* (SVLAC), and *Amycolatopsis* (AMLAC). The genes encoding the small laccases from *S. coelicolor* A3(2) (GI 21225006), *S. lividans* TK24 (GI 256783840), *S. viridosporus* T7A (GI 2518361192), and *Amycolatopsis* sp. 75iv2 (GI 2513525025) were amplified via PCR from their corresponding genomic DNA without a TAT secretion tag, with the primers (Integrated DNA technologies) listed in Table S1 of the Supporting Information, all of which had a 5′-NdeI restriction site and a 3′-BamHI restriction site, respectively. The PCR mixture (50 μL) contained 5 μL of 5 ng/μL template genomic DNA, 10 μL of Expand High Fidelity^{PLUS} reaction buffer (5×) with 7.5 mM $MgCl_2$, 2 μL of a 10 mM dNTP mixture, 2.5 μL of DMSO, 2 μL of 20 μM forward primer, 2 μL of 20 μM reverse primer, 1 μL of Expand High Fidelity^{PLUS} (5 units/μL) enzyme blend (Roche), and 25.5 μL of ddH_2O. The PCRs were performed in a Veriti 96 Well Thermal Cycler (Applied Biosystems) with the following parameters: 94 °C for 4 min followed by 35 cycles of 94 °C for 30 s, 70 °C for 45 s, and 72 °C for 1.15 min, and a final extension time of 7 min at 72 °C. The PCR products were purified by gel extraction (Qiagen) following the manufacturer's protocol. The amplified DNA products were digested with NdeI and BamHI restriction enzymes (New England Biolabs) and ligated into the pET15b expression vector (Novagen) cut with the same enzymes. The N-terminally His-tagged proteins were expressed in *E. coli* BL21(DE3) cells at 30 °C. A bacterial culture for a typical preparation utilized 4 × 1 L of LB medium shaken at 37 °C until the OD_{600} reached 0.6, after which it was induced with 1 mM IPTG. The culture was then shaken at 30 °C for an additional 20 h and harvested by centrifugation. The cell pellets were resuspended in 50 mL of buffer containing 5 mM imidazole, 500 mM NaCl, and 20 mM Tris-HCl (pH 7.9). The suspension was sonicated to lyse the cells, and the lysate was cleared by centrifugation. The supernatant was applied to a 5 mL HisTrap HP column (GE Healthcare) and eluted with a linear gradient (100 mL) of 0 to 1 M imidazole buffered with 500 mM NaCl and 20 mM Tris-HCl (pH 7.9). Fractions containing the small laccase were collected and dialyzed against 1× PBS (phosphate-buffered saline) (pH 7.4) containing 137 mM NaCl, 2.7 mM KCl, 10 mM Na_2HPO_4, and 1.76 mM KH_2PO_4. After cleavage of the N-terminal His tag by thrombin (GE Healthcare) at room temperature, the proteins were dialyzed against 20 mM Tris-HCl (pH 7.9) before being applied to a 5 mL HiTrap Q HP column (GE Healthcare). The proteins were eluted with a linear gradient (100 mL) from 0 to 1 M NaCl buffered with 20 mM Tris-HCl (pH 7.9). Fractions containing pure (>95%) proteins were collected and dialyzed twice against 20 mM Tris-HCl (pH 7.9) containing $CuSO_4$ at a 4-fold greater molar ratio to give four copper atoms per active site and then stored at −80 °C.

Determination of Laccase Activity at Different pH Values. The small laccase activities at different pH values (3−10) were determined at 25 °C using 2,2′-azinobis(3-ethylbenzothiazoline-6-sulfonate) (ABTS) or 2,6-dimethoxyphenol (DMP) as the substrate. The oxidation of substrates was detected by measuring the absorbance at 420 nm for ABTS (ε_{420} = 36000 M^{-1} cm^{-1}) at pH 3−5 and 468 nm (ε_{468} = 14800 M^{-1} cm^{-1}) for DMP at pH 6−10. The reaction mixture (200 μL) contained 10 mM ABTS (dissolved in water), 5 mM DMP (dissolved in DMF), and the small laccase (2.0 μM) with the appropriate buffer.

Determination of k_{rel} and K_{app} Values of Small Laccases. LM-OH, a phenolic β-O-4 lignin model compound

dx.doi.org/10.1021/bi500285t | *Biochemistry* 2014, 53, 4047−4058

Table 1. Data Collection and Refinement Statistics for AMLAC

	AMLAC·Cu^{2+}·LM-OMe	AMLAC·Cu^{2+}
Data Collection		
space group	$C222_1$	$R32$
no. of molecules in the asymmetric unit	3	1
cell dimensions		
a, *b*, *c* (Å)	84.42, 115.26, 163.51	110.180, 110.180, 178.820
α, *β*, *γ* (deg)	90.00, 90.00, 90.00	90.00, 90.00, 120.00
resolution (Å)	19.80−2.35 (2.41−2.35)	19.85−1.50 (1.54−1.50)
no. of unique reflections	33545	66783
R_{merge}	0.101 (0.641)	0.078 (0.619)
$I/\sigma I$	20.65 (2.71)	18.46 (2.6)
completeness (%)	99.8 (99.8)	99.9 (100.0)
Refinement		
resolution (Å)	19.80−2.35	19.66−1.50
R_{cryst}	0.176	0.172
R_{free}	0.238	0.202
root-mean-square deviation		
bond lengths (Å)	0.008	0.008
bond angles (deg)	1.408	1.389
no. of atoms		
protein	6455	2192
water	264	468
substrate	24	−
metal ion	15	5
B factor		
Wilson plot	29.8	18.0
protein	29.7	20.1
ligand	39.3	27.5
solvent	27.8	35.4
PDB entry	3TA4	3T9W

(Figure S2 of the Supporting Information), was used as lignin model substrate to determine the k_{rel} and K_{app} of small laccases. Spectrophotometric assays were performed at room temperature and monitored at 340 nm [ε_{340} = 1500 M^{-1} cm^{-1} for the formation of vanillin, one of the LM-OH oxidation products (Figure S9 of the Supporting Information)]. Reaction mixtures (200 μL) were buffered at varying pH values (6−10) with 100 mM potassium phosphate buffer (pH 6−8) and 100 mM sodium carbonate buffer (pH 9−10). It contained 1−100 mM LM-OH (dissolved in DMF) as a substrate and the enzyme (20−30 μM) at room temperature. The steady-state kinetic parameters were evaluated by fitting the initial rates to the Michaelis−Menten equation using GraphPad Prism.[36]

Ethanosolv Lignin Degradation by Small Laccase. To detect the activity of the small laccase with a heterogeneous mixture of lignin building blocks, the enzyme was incubated for 16 h in the presence of ethanosolv lignin. The resultant cloudy reaction mixture with some precipitate was mixed vigorously while an equal volume of 20% acetonitrile (CH_3CN) in water was added to a final concentration of 10% to produce a homogeneous suspension. The mixture containing 10% CH_3CN was then centrifuged for 10 min at 15000*g*. The cleared supernatant was applied to a C18 column (μBondapak C18, 10 μm, 125 Å, 4.6 mm × 150 mm, Waters) and eluted with a 10% isocratic CH_3CN/H_2O gradient for 5 min, followed by a linear gradient from 10 to 60% for 25 min at a flow rate of 1 mL/min, and monitored at 285 nm.

Size exclusion chromatography was utilized to elucidate the relative size distribution of small laccase-degraded ethanosolv lignin. For size exclusion, the cloudy reaction mixture was mixed with an equal volume of a 60% CH_3CN/H_2O mixture to solubilize the otherwise insoluble lignin species. A sample (20 μL) was then injected into the size exclusion column (BioSuite 125, 4 μm UHR SEC, 4.6 mm × 300 mm, Waters) with a mobile phase consisting of a 30% CH_3CN/H_2O mixture, eluted at 0.4 mL/min, and monitored at 315 nm.

Crystallization and Data Collection for AMLAC. Two crystal forms of the *Amycolatopsis* sp. 75iv2 small laccase (AMLAC) were obtained utilizing the Hampton Research sparse matrix crystallization screens. Crystals were obtained in the presence and absence of a nonphenolic *β*-O-4 lignin model compound (LM-OMe) (Figure S2 of the Supporting Information). Both crystal forms appeared within 2 weeks of the initial setup under Crystal Screen II condition #3 and Index Screen condition #11. Centered orthorhombic crystals were obtained in the presence of the LM-OMe substrate analogue in the first and rhombohedral ligand-free crystals in the second condition using the hanging drop vapor diffusion method at 4 °C.

For the AMLAC·Cu^{2+}·LM-OMe crystals [Protein Data Bank (PDB) entry 3TA4], the protein solution contained AMLAC (20 mg/mL) in 20 mM Tris-HCl (pH 7.9) and 20 mM LM-OMe ligand; the precipitant contained 25% ethylene glycol. Crystals appeared within 2 weeks and exhibited diffraction consistent with space group $C222_1$, with three molecules per asymmetric unit. Prior to data collection, the crystals were dipped in fresh mother liquor and then flash-cooled in liquid nitrogen; the ligand was not included in the cryoprotectant solution.

Table 2. Data Collection and Refinement Statistics for SVLAC

	SVLAC·Cu^{2+}·Zn^{2+}	SVLAC·Cu^{2+}	SVLAC·Cu^{2+}·AV
	Data Collection		
space group	*I*222	$P3_121$	$P3_121$
no. of molecules in the asymmetric unit	3	3	3
cell dimensions			
a, *b*, *c* (Å)	102.30, 157.18, 162.33	127.00, 127.00, 155.07	127.02, 127.02, 155.54
α, *β*, *γ* (deg)	90.00, 90.00, 90.00	90.00, 90.00, 120.00	90.00, 90.00, 120.00
resolution (Å)	19.69−2.30 (2.36−2.30)	29.93−2.3 (2.38−2.30)	19.76−2.7 (2.77−2.70)
no. of unique reflections	58241	64657	40270
R_{merge}	0.20 (0.797)	0.164 (0.786)	0.157 (0.861)
$I/\sigma I$	10.51 (2.02)	15.12 (2.23)	15.42 (2.20)
completeness (%)	99.8 (99.9)	99.9 (100.0)	99.6 (99.9)
	Refinement		
resolution (Å)	19.69−2.30	29.93−2.3	19.76−2.70
R_{cryst}	0.147	0.161	0.157
R_{free}	0.193	0.206	0.210
root-mean-square deviation			
bond lengths (Å)	0.008	0.008	0.008
bond angles (deg)	1.269	1.342	1.275
no. of atoms			
protein	6918	6450	6428
water	615	563	313
substrate	−	−	12
metal ion	18	12	12
B factor			
Wilson plot	21.0	32.6	43.9
protein	22.1	31.9	46.7
ligand	20.6	39.4	64.3
solvent	29.9	36.8	41.9
PDB entry	3TBB	3TAS	3TBC

For the AMLAC·Cu^{2+} crystals (PDB entry 3T9W), the protein solution contained AMLAC (20 mg/mL) in 20 mM Tris-HCl (pH 7.9); the precipitant contained 3.0 M NaCl and 100 mM Hepes (pH 7.5). Crystals appeared within 2 weeks and exhibited diffraction consistent with space group *R*32, with one molecule per asymmetric unit. Prior to data collection, the crystals were immersed in a cryoprotectant solution composed of 30% glycerol and 70% original mother liquor. After being incubated for 30 s, the crystals were vitrified by immersion in liquid nitrogen.

The diffraction data for AMLAC·Cu^{2+} crystals were recorded at LS-CAT (Sector 21 ID-G, Advanced Photon Source, Argonne, IL) using a MAR 300 CCD detector. The diffraction data for AMLAC·Cu^{2+}·LM-OMe crystals were recorded at LS-CAT (Sector 21 ID-F, Advanced Photon Source) using a MAR 225 CCD detector. Diffraction intensities were integrated and scaled with the XDS package.[37] Relevant data collection and data reduction statistics are listed in Table 1.

Crystallization and Data Collection for SVLAC. Two crystal forms were also obtained for the *S. viridosporus* T7A small laccase (SVLAC). Approximately 1 month after the initial setup of the Precipitant Synergy sparse matrix screen, orthorhombic crystals appeared under condition #16 and trigonal crystals under condition #8 using the hanging drop vapor diffusion method at 9 °C. The trigonal crystal form was also subjected to soaking experiments with acetovanillone (AV), a naturally occurring mediator.[38,39] Although cocrystallization with the LM-OMe compound was attempted, no ligand was detected in resultant electron density maps for either of the two crystal forms. The presence of the Zn^{2+} atom in the first crystal form was established via the identities of its binding residues.[40] In addition, the zinc content of the enzyme was analyzed with Sciex Elan DRCe ICP-MS (PerkinElmer) at the University of Illinois Microanalytical Laboratory.

For the SVLAC·Cu^{2+}·Zn^{2+} crystals (PDB entry 3TBB), the protein solution contained SVLAC (20 mg/mL) in 50 mM Hepes-K^+ (pH 8.0) and 100 mM KCl; the precipitant contained 2.0 M Li_2SO_4, 5% poly(ethylene glycol) 400, 100 mM $MgSO_4$, and 100 mM acetate (pH 5.5). Crystals appeared in approximately 1 month and exhibited diffraction consistent with space group *I*222, with three molecules per asymmetric unit. Prior to data collection, the crystals were immersed in a cryoprotectant solution composed of 4.0 M sodium malonate. After being incubated for 30 s, the crystals were vitrified by immersion in liquid nitrogen.

For the SVLAC·Cu^{2+} crystals (PDB entry 3TAS) and SVLAC·Cu^{2+}·AV crystals (PDB entry 3TBC), the protein solution contained SVLAC (20 mg/mL) in 20 mM Tris-HCl (pH 7.9); the precipitant contained 5% 2-propanol and 2.5 M dibasic potassium phosphate/monobasic sodium phosphate (pH 5.5). Crystals appeared in approximately 1 month and exhibited diffraction consistent with space group $P3_121$, with three molecules per asymmetric unit. Prior to data collection, the SVLAC·Cu^{2+} crystals were immersed in a cryoprotectant solution composed of 70% original mother liquor and 30% glycerol. After being incubated for 30 s, the crystals were vitrified by immersion in liquid nitrogen. For SVLAC·Cu^{2+}·AV crystals, the ligand-free crystals were transferred into fresh mother liquor containing 20 mM acetovanillone and incubated

dx.doi.org/10.1021/bi500285t | *Biochemistry* 2014, 53, 4047−4058

at 9 °C for 4 h. The crystals were vitrified as described above, and the cryoprotectant solution did not contain the ligand.

The diffraction data for SVLAC·Cu^{2+}·Zn^{2+} crystals were recorded at LS-CAT (Sector 21 ID-G, Advanced Photon Source) using a MAR 300 CCD detector. The diffraction data for SVLAC·Cu^{2+} and SVLAC·Cu^{2+}·AV crystals were recorded at LS-CAT (Sector 21 ID-F, Advanced Photon Source) using a MAR 225 CCD detector. Diffraction intensities were integrated and scaled with the XDS package.[37] The data collection statistics are listed in Table 2.

Structure Determination and Model Refinement for AMLAC and SVLAC. The structures of both liganded and unliganded AMLAC and SVLAC were determined by molecular replacement with PHASER,[41] using the atomic coordinates of the small laccase from *S. coelicolor* A3(2) (PDB entry 3CG8) as the search model. The partial solution from PHASER was then subjected to automated model building with ARP/wARP,[42] followed by multiple iterative cycles of manual and automated rebuilding with COOT,[43] interspersed with rounds of refinement using PHENIX.[44] Water molecules were automatically built with ARP/wARP, followed by manual assessment in COOT. Final refinement statistics are listed in Tables 1 and 2.

RESULTS AND DISCUSSION

Identification of the Small Laccase. The genome of *S. coelicolor* A3(2) encodes a "small" laccase (SCLAC) that is homologous to fungal laccases, although the bacterial laccase contains two domains and the larger fungal laccases contain three domains. The gene encoding SCLAC is genome proximal (separated by eight genes) to a seven-gene operon encoding enzymes in the β-ketoadipate pathway to the tricarboxylic acid cycle intermediates acetyl-CoA and succinyl-CoA.[45] Homologous gene clusters can be found in the genomes of several *Streptomyces* species, including *S. lividans* TK24, *Amycolatopsis* sp. 75iv2, and *S. griseus* NBRC 13350. Because lignin is composed of aromatic moieties, we investigated whether SCLAC is involved in lignin degradation[24,31] by disruption of the gene encoding the small laccase by insertion of an apramycin resistance cassette, *apr*, using the PCR-targeted *Streptomyces* gene replacement method, yielding the mutant designated SCΔLAC.

Lignocellulose Degradation by the Small Laccase. Quantitative studies of lignin degradation are hampered by the lack of convenient assay methods because of the complexity and heterogeneity of its polymeric structure (Figure S1 of the Supporting Information). The mineralization of lignin can be quantified by the conversion of ^{14}C-labeled lignin to $^{14}CO_2$. However, this method requires the biosynthetic preparation of the isotopically labeled substrate and, therefore, may allow for the incorporation of radioactivity into non-lignin components of the lignocellulose, e.g., proteins, aromatic acids esterified to hemicelluloses or to lignin, and other aromatics such as lignans.[8] Also, a spectrophotometric assay recently was reported using chemically nitrated lignin; but the assay sensitivity is low, and we were unable to demonstrate lignin degradation using this method.[46] Monomeric and β-O-4 dimeric lignin model compounds have been used, but these are not perfect representations of the complex native lignin structures.[47] Finally, some organisms show lignin degradation activity only in the presence of cellulosic biomass, i.e., in the native lignocellulosic state.[48] Therefore, we considered the use of native lignocellulose, a combination of lignin, cellulose, and hemicellulose, as an important real-world criterion for determining the lignin degradation activity of microorganisms.

Considering the molecular size and structure of lignin, it is reasonable to postulate that its microbial degradation will involve extracellular (secreted) enzymes. Actinomycetes are known to secrete enzymes that produce water-soluble, polymeric lignin fragments from different lignocellulosic materials. These intermediates precipitate from aqueous solution upon acidification and are known as acid-precipitable polymeric lignin (APPL).[35] Quantification of APPL production can provide a measure of the lignin degradation efficiency; chemical characterization of the APPL has the potential to elucidate the molecular processes involved in lignin degradation.[35] We reasoned that if the small laccase is involved in lignin degradation, less APPL would be produced by the SCΔLAC mutant than by the wild-type SCWT strain. Also, chemical analysis of the APPL produced by the mutant and wild-type strains would provide a measure of the extent of lignin degradation and therefore the importance of the small laccase in APPL production.

APPL production assays were performed with the SCWT and SCΔLAC mutant strains using milled, air-dried lignocellulose from *Miscanthus x giganteus* as the source of the lignin substrate.[3] Controls were performed using (i) the medium alone, (ii) the medium with lignocellulose, and (iii) the medium with either the SCWT or SCΔLAC mutant strain in the absence of lignocellulose. The growth of SCWT and SCΔLAC mutant strains was similar under experimental conditions (the growth was measured by monitoring the OD at 600 nm). After incubation for 1 week, the residual lignocellulose and bacteria were removed by centrifugation. The supernatants were acidified at 4 °C to minimize acid hydrolysis, and the resulting precipitates (APPL) were dried and weighed. APPL was found in the supernatants of the cultures containing both bacteria and lignocellulose but not in any of the control experiments (Figure 1). This indicates that

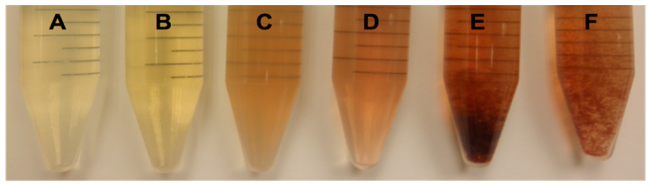

Figure 1. Results of APPL experiments with (A) medium alone, (B) medium with lignocellulose, (C) medium with wild-type *S. coelicolor* A3(2) (SCWT), (D) medium with a laccase deficient mutant (SCΔLAC), (E) medium with both lignocellulose and SCWT, and (F) medium with both lignocellulose and SCΔLAC.

APPL is the breakdown product of lignocellulosic substrates in the presence of the SCWT and SCΔLAC mutant strains and not a hydrolysis product of lignocellulose.

Although the SCΔLAC strain produced APPL, the total amount of APPL was significantly smaller (33.1%) than that produced by the wild-type strain (Table 3). The fact that the mutant was deficient in APPL production may support the possible importance of the small laccase in lignin degradation. The results of the compositional characterization and chemical analysis of the APPLs produced by the SCWT and SCΔLAC strains are listed in Table 4. The results are means of triplicate analysis, except for ash (duplicate analysis) and nitrogen (single analysis). The level of lignin degradation (Klason lignin) as

Table 3. APPL Production by Wild-Type *S. coelicolor* A3(2) (SCWT) and Its Laccase Deficient Mutant (SCΔLAC)

	APPL production (mg) in cultures	
culture	SCWT	SCΔLAC
1	155	103.5
2	161.4	108.5
3	160.6	107

Table 4. Compositional Analysis of APPL

compound	SCWT (mg)	SCΔLAC (mg)
glucan	6.87 ± 0.20	5.13 ± 0.10
xylan	6.74 ± 0.06	4.25 ± 0.02
arabinan	2.28 ± 0.07	2.51 ± 0.03
acetyl	1.58 ± 0.06	0.67 ± 0.03
Klason lignin	155 ± 6	68.6 ± 4.0
ash	83.1 ± 0.6	80.7 ± 0.7
nitrogen	32.43	30.89

measured from the total amount of APPL produced by SCWT was much greater than that produced by the SCΔLAC strain (Table 4). As a result of the larger extent of lignin degradation by the SCWT strain, a larger amount of carbohydrate (glucan, xylan, and arabinan) was released by the SCWT strain (15.9 mg) than by the SCΔLAC strain (11.9 mg), suggesting the hydrolytic enzymes had easier access to the carbohydrate biomass. The acetyl content of the APPL quantitates the acetyl released from acetyl esters of both lignin and hemicellulose; the larger amount of acetyl released by the SCWT strain again suggests greater accessibility to the carbohydrate biomass because of the greater lignin degradation by the SCWT strain. Ash and nitrogen measure the amounts of inorganic salts and protein present in APPL, respectively, and were unchanged by the disruption of the gene encoding the small laccase (Table 4).

Functional Characterization of Purified Small Laccases. To investigate further the involvement of small laccases in lignin degradation, four small laccase enzymes, SCLAC, SLLAC, SVLAC, and AMLAC, were expressed and purified from *E. coli* with a high yield (15–20 mg/L of cell culture). Sodium dodecyl sulfate–polyacrylamide gel electrophoresis (SDS–PAGE) of pure laccase enzymes shows both monomeric and trimeric forms, an observation found previously (Figure S8 of the Supporting Information).[24] They are very stable enzymes that are active across a broad pH range (3–10), compared to fungal laccases that are mostly active at low pH.[49,50] Their activities were determined using ABTS (pH 3–5) and DMP (pH 6–10) as substrates (data not shown). The high yields of the small laccases from *Streptomyces* using *E. coli* as heterologous expression system and their stability over a broad pH range make them excellent candidates for various industrial applications.

Oxidative Degradation of Lignin Model Compounds. Both phenolic and nonphenolic dimeric β-O-4 lignin model compounds are widely used to study C_α–C_β bond cleavage in lignin degradation.[8] The ability of small laccases to degrade and/or oxidize the dimeric β-O-4 lignin model compounds indirectly reflects their lignin oxidative degradation ability, as more than 50% of lignin structure is composed of β-O-4 bonds.[3] Scheme S1 of the Supporting Information demonstrates a possible oxidative degradation pathway of β-O-4 lignin model compounds by laccases. It was postulated that laccase is responsible for only the radical initiation step, with the downstream C–C bond deconstruction the result of spontaneous reactions.[51] The catalytic activities of the *Streptomyces* laccases were determined by measuring the release of degradation product(s) because of the C_α–C_β bond cleavage and/or rearrangement of the LM-OH phenolic β-O-4 lignin model compound at pH 8.0 and 25 °C. A mixture of oxidative degradation products was formed, which were not fully characterized. However, one of the products was identified and characterized as vanillin, which absorbs at 340 nm (Figure S9 of the Supporting Information). The formation of product(s) at this wavelength was found to show Michaelis–Menten kinetics, and thereby, the relative k_{cat} (k_{rel}) and apparent K_M (K_{app}) values were calculated for small laccases (Table 5). The low k_{rel}/K_{app} (low k_{rel} and high K_{app}) values

Table 5. Steady-State Kinetic Parameters for the Laccases with LM-OH at pH 8.0

enzyme	k_{rel} (min^{-1})	K_{app} (mM)	k_{rel}/K_{app} (min^{-1} mM^{-1})
SCLAC	26 ± 2	102 ± 14	(25 ± 1) × 10^{-2}
SLLAC	29 ± 3	120 ± 17	(24 ± 2) × 10^{-2}
SVLAC	39 ± 2	143 ± 10	(27 ± 2) × 10^{-2}
AMLAC	10 ± 1	133 ± 7	(8 ± 1) × 10^{-2}

suggest that the β-O-4 model compound is not the natural substrate, prompting us to use the slightly modified native lignin substrate (ethanosolv lignin) for further studies. The pH optimum for SCLAC against LM-OH was determined; the values of k_{rel} and k_{rel}/K_{app} were highest at pH 8.0 (Figure S3 of the Supporting Information). Different mediators, ABTS and HOBt, were used to oxidize the nonphenolic β-O-4 lignin model compound (LM-OMe) in the presence of small laccases. No C_α–C_β bond cleavage was observed; instead, there was very slow formation of the corresponding ketone product [Figure 2,

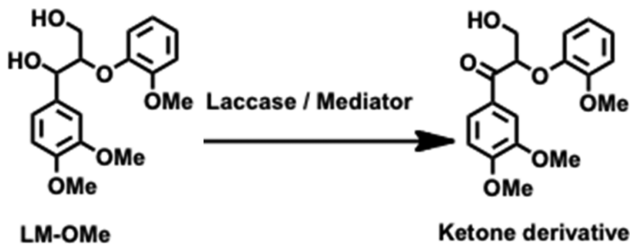

Figure 2. Oxidation of the nonphenolic β-O-4 lignin model compound (LM-OMe) in the presence of laccase and a mediator to the corresponding ketone derivative.

identified by MS (Figure S7 of the Supporting Information)], a behavior previously observed with fungal laccase.[52] However, the rate of conversion of LM-OMe to the quinone product by small laccases was slower compared to that of fungal laccase from *T. versicolor* (data not shown). This result suggests that even in the presence of mediators neither bacterial nor fungal laccases were able to cleave the C_α–C_β bond of LM-OMe, but they were able to modify the structure by forming the quinone product at different rates. These activities explain the role of laccases in enhancing the access of energy rich cellulose and hemicellulose by modifying lignin structure.[16]

Degradation and/or Modification of Ethanosolv Lignin. To verify the activity of the laccases against native lignin, ethanosolv lignin was used because of its better water solubility. Ethanosolv lignin was prepared by pretreating native

dx.doi.org/10.1021/bi500285t | *Biochemistry* 2014, 53, 4047–4058

Miscanthus lignocellulose with 80% aqueous ethanol and 0.5% (w/w) (based on raw material dried mass) sulfuric acid as a catalyst at high temperatures.[2,32] Ethanosolv lignin retains the same lignin and carbohydrate composition as native lignocellulose except that the molecular weight is lower, which makes it more water-soluble and convenient for enzyme assays.[2] After ethanosolv lignin had reacted with purified SCLAC for 16 h at 37 °C, the reaction mixture was passed through a reverse phase C18 column; the elution profile is shown in Figure 3. As

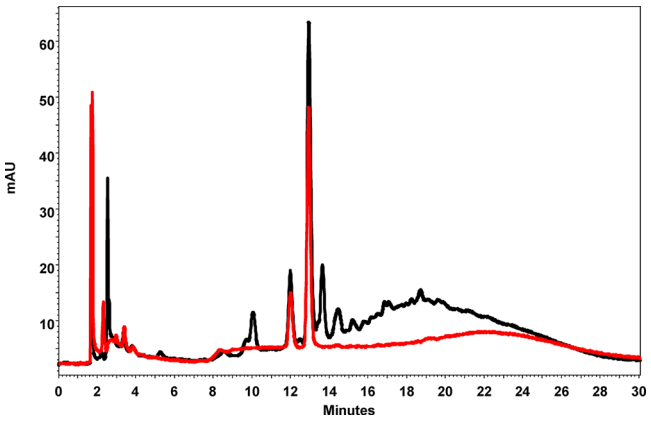

Figure 3. Reverse phase chromatography of the soluble fraction of ethanosolv lignin. The black line is for the starting material. The red line is for ethanosolv lignin reacted with SCLAC for 16 h at 37 °C.

determined by LC−MS, most of the ionizable peaks from this elution profile belong to a molecular weight range of 200−1000 Da. The major species (~13 min) was determined, by Agilent 1100 LC/MSD Trap XCT Plus (LC−MS) at the University of Illinois Roy J. Carver Biotechnology center, to be *p*-coumaric acid ethyl ester with a molecular weight of 192.08 Da, an expected lignin degradation product and a natural laccase mediator.[53,54] The chromatogram seems to indicate the loss of soluble material, which can be equated to polymerization of the smaller lignin units into larger pieces that are less soluble in aqueous solution and were not retained during workup on the reaction mixture for C18 chromatography (*vide infra*). It is believed that laccases catalyze the oxidation of lignocellulosic substrates to produce aryl cation radicals; these radicals spontaneously rearrange, leading to further polymerization of degraded materials by the fission of carbon−carbon or carbon−oxygen bonds of the alkyl side chains or to the cleavage of aromatic rings.[55,56] When this was taken into account, our experiments that aimed to reproduce natural lignin biodegradation *in vitro* indicate that although the laccase is able to degrade lignin substrates, the products simultaneously undergo competing radical polymerization.

To probe this conclusion, we used size exclusion chromatography to elucidate the relative size distribution of ethanosolv lignin after reaction with SCLAC. The results are shown in Figure 4. For this experiment, unlike the reverse phase C18 column chromatography experiment, the cloudy reaction mixture was mixed with an equal volume of a 60% CH_3CN/H_2O mixture to solubilize the polymerized lignin species. An observable shift toward higher-molecular weight lignin was observed, as was expected on the basis of the loss of material in the C18 chromatograms (*vide supra*). Because of the lack of appropriate molecular weight standards, the molecular weight estimate is only qualitative. Nevertheless, we can

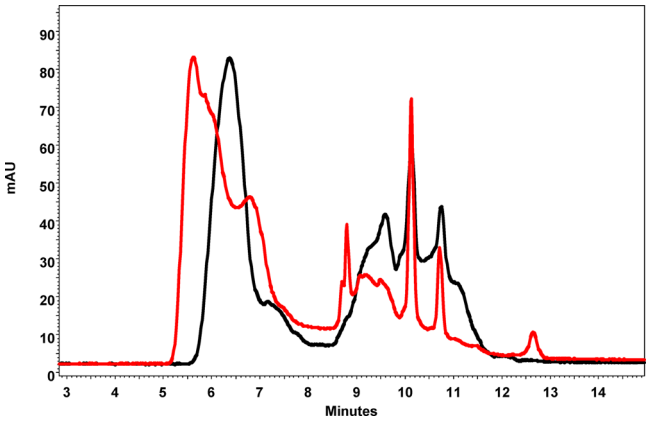

Figure 4. Size exclusion chromatography of ethanosolv lignin. The mobile phase was a 30% CH_3CN/H_2O mixture. The black trace is for unreacted ethanosolv lignin. The red trace is for ethanosolv lignin that was reacted with SCLAC at 37 °C for 16 h.

conclude that during *in vitro* lignin degradation there is competition between depolymerization and repolymerization, which would shift toward depolymerization under *in vivo* conditions because of the presence of a suitable radical quencher.[56] Considering the very complex structure of lignin and the subsequent complexity of recondensation of reactive lignin degradation products, it is unlikely that this biopolymer can be effectively degraded by one enzyme alone. In fungi, FAD-dependent enzymes veratryl alcohol oxidase and glucose 1-oxidase were considered to have cooperative action with laccase to prevent the repolymerization by reducing the reactive radical species.[51,56] For *Streptomyces*, the discovery of such a cooperative enzyme for the prevention of repolymerization is an area of active study.

Structure of Small Laccases. A multiple-sequence alignment of all four small laccases shows that all the active site residues involved in copper binding are conserved (Figure S4 of the Supporting Information). These residues are also highly conserved among other laccases and four-copper oxidases from fungi, plants, and bacteria, although there is less similarity across the rest of the protein.[24]

Laccases are known to bind four copper(II) ions in three different binding sites, each characterized by unique spectroscopic properties and playing an important role in substrate oxidation.[31,57−60] The paramagnetic type 1 (T1) copper is coordinated by two His residues, one Met residue, and one Cys residue. The tight coordination of T1 copper to the Cys residue is responsible for an intense absorption band around 600 nm, giving the blue color to the enzyme. Two His residues are coordinated to one paramagnetic type 2 (T2) copper, and three His residues (six His residues total) are coordinated to each of the two type 3 (T3) coppers. The T3 coppers are antiferromagnetically coupled with the EPR silent pair absorption maximum at 330 nm. The one T2 copper and two T3 coppers are arranged in a trinuclear cluster, which is believed to be the site of molecular oxygen reduction.[31,57] The catalytic cycle is thought to be initiated by oxidation of the substrate near the T1 copper site by transfer of an electron from the substrate. In total, four electrons (produced by oxidation of four substrates) are then sequentially transferred from the T1 copper to the trinuclear cluster along a Cys-His pathway, where one oxygen molecule is reduced to two water molecules to complete the cycle.[31]

dx.doi.org/10.1021/bi500285t | *Biochemistry* 2014, 53, 4047−4058

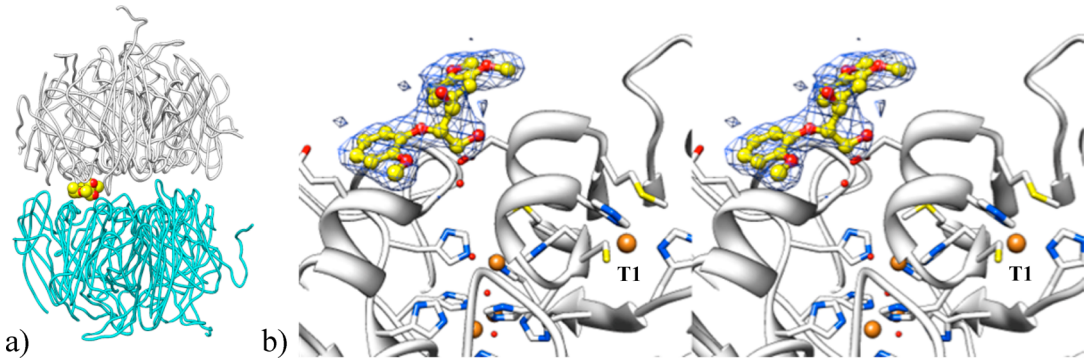

Figure 5. (a) Two trimers related by crystallographic symmetry create a wedge in the AMLAC structure, which allows ligand binding on one side of the trimer−trimer interface. (b) Stereoview of ligand binding. The electron density for the ligand molecule is contoured at 2.5σ on a difference $F_o - F_c$ omit map; T1 designates the mononuclear copper center.

The structure of AMLAC was determined in the presence (PDB entry 3TA4) and absence (PDB entry 3T9W) of a noncleavable lignin β-O-4 model compound LM-OMe (Figure S2 of the Supporting Information). Although the biologically active form of the enzyme is a trimer, the ligand-free structure (space group *R*32) contains one molecule per asymmetric unit. In this case, the crystallographic symmetry-related molecules complete the trimeric composition. To date, the unliganded structure of AMLAC reported here (PDB entry 3T9W) is the highest-resolution structure of a small bacterial laccase. The sequence of the enzyme is 58% identical to those of the previously reported small laccase from *S. coelicolor* A3(2) (PDB entries 3CG8 and 3KW8) (SCLAC) and consists of an identical two-domain fold with metal binding architecture.[31]

The T1 copper binding site contains a highly ordered copper ion that is coordinated to Cys 279, His 222, and His 284 with Met 298 as the axial ligand. The T2 copper is coordinated to His 93 and *His 225 (where the asterisk denotes the residue from a symmetry-related polypeptide). The first T3 copper is coordinated to His 95, His 147, and *His 280; the second T3 copper site consists of His 149, *His 278, and *His 227. The area between the T2 and T3 copper centers contains strong positive electron density in the $F_o - F_c$ omit map, suggestive of a bound dioxygen molecule. However, the electron density is elongated so a hydrogen peroxide molecule may be more appropriate. This dioxygen reduction intermediate, however, is not unusual and has previously been reported in three-domain laccase structures with almost identical coordination geometry (Figure S5 of the Supporting Information).[61,62]

Whereas the three-domain laccases contain a negatively charged Glu or Asp residue in the tip of the access solvent channel, the water molecule coordinated to O1 of the peroxide is bonded to a polar Gln 282 residue in the AMLAC structure. The ligand-bound structure of AMLAC (PDB entry 3TA4, space group $C222_1$) contains three polypeptides in the asymmetric unit. The trimer contains three trinuclear and three mononuclear copper centers. Serendipitously, this crystal form allows for the binding of the nonphenolic lignin model compound LM-OMe, which was included in the crystallization solution. Although the surface of the trimer lacks defined cavities that may act as the binding pocket for small-molecule phenolic substrates, it is conceivable that the rather flat trimer surface is optimal for binding large phenolic polymers. Although it is questionable whether the binding of the model compound is biologically relevant, its binding site is close to the T1 copper site, which is believed to be the main source of catalytic activity for the oxidation of phenolic compounds.[63,64] The ligand in this crystal form is trapped in a "wedge" between two crystallographic symmetry-related trimers (Figure 5). It is also not possible to assess the orientation of the inert substrate molecule because of its three-dimensional conformation, which is nearly symmetric (Figure 5). The ligand was modeled at an occupancy of 0.46 as the molecule lies on a symmetry axis and occupies approximately half of the site. The site lying between the T2 and T3 copper atoms that was occupied by a hydrogen peroxide moiety in the ligand-free structure contains a water molecule.

Structures of SVLAC were determined in two distinct crystal forms. The sequence of SVLAC is 87% identical to that of SCLAC and differs mainly in the sequence of the C-terminal tail of the enzyme. Both crystal forms are composed of asymmetric units that contain the biologically active trimeric enzyme. However, regions that were ordered in the crystal form belonging to *I*222 space groups were disordered in the crystals belonging to the $P3_121$ space group because of crystal packing. However, the hexagonal crystal form produced a condition similar to that of the trimeric form of AMLAC, allowing the trapping of a substrate molecule at the crystallographic symmetry-related trimer interface. The new feature that can be observed with the structure belonging to the *I*222 space group is the extra metal binding site (PDB entry 3TBB), which arises from an insertion of two extra histidine residues at the C-terminus that SCLAC lacks.

On the basis of the results from the ICP-MS analysis, we hypothesize that this site contains a zinc ion. The binding pocket for the zinc ion is formed by Glu 158 and His 159 of one polypeptide and a *His 315 residue of the neighboring polypeptide. In all three zinc binding sites in the trimer, the metal ion is within ∼2.3 Å of the ϵ-nitrogen of the histidine residues and within ∼2.6 Å of the carboxylate oxygen of the glutamate moiety. In each of the three sites, the zinc ion is also coordinated to at least one water molecule (Figure S6 of the Supporting Information).

In the structure, the mono- and trinuclear copper sites are conserved. The T1 copper binding site contains a highly ordered copper ion that is coordinated to Cys 283, His 226, and His 288 with Met 293 as the axial ligand. The T2 copper is coordinated to His 97 and *His 229. The first T3 copper is coordinated to His 99, His 151, and *His 284; the second T3 copper site consists of His 153, *His 282, and *His 231. The site that was occupied by a hydrogen peroxide in the high-resolution structure of AMLAC contains a dioxygen molecule

dx.doi.org/10.1021/bi500285t | *Biochemistry* 2014, 53, 4047−4058

in all three polypeptides of SVLAC. Interestingly, a molecule of acetate, a component of the crystallization buffer, is coordinated to one of the T3 copper atoms in all three polypeptides. The trigonal crystal form, which lacks the C-terminal tail involved in zinc coordination, was an excellent candidate for soaking experiments.

Although multiple natural mediators were tested in soaking experiments, only acetovanillone (AV) yielded detectable electron density in the resultant structure. Although the presence of AV is again most likely attributable to crystal packing, this phenolic substrate is bound only ~10 Å from the T1 copper site. The binding of AV, when compared to the binding of LM-OMe to AMLAC, seems to be more specific with multiple hydrogen bonding interactions with the SVLAC polypeptide. The molecule of AV is stacked against what appears to be a molecule of Tris from the purification buffer (Figure 6). The Tris, however, is ordered only in the liganded structure and is missing from the electron density in the apo form of this crystal form.

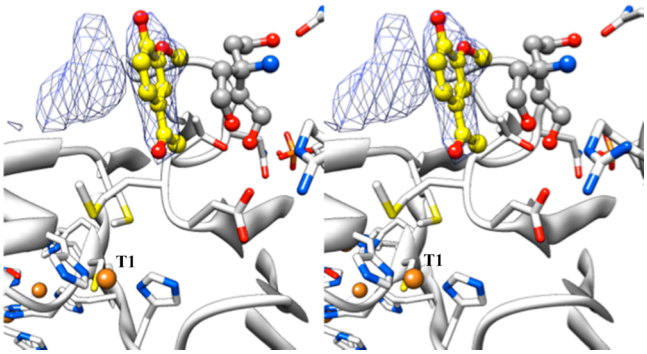

Figure 6. Stereoview of the binding geometry of acetovanillone in SVLAC. Electron density for acetovanillone is shown on a difference $F_o - F_c$ omit map contoured at 3σ. The unoccupied density belongs to the symmetry-related molecule of acetovanillone, which is not shown here. T1 denotes the mononuclear copper center.

CONCLUSIONS

We provided evidence that (1) strains of *Streptomyces* that encode the small laccase have the potential to be useful in lignin degradation and (2) the extracellular small laccase plays an important role in this process. The small laccases from four different *Streptomyces* species were cloned, expressed, and purified from heterologous sources and proved to be stable and active against different substrates under various pH conditions. These enzymes were able to degrade the phenolic β-O-4 lignin model compound without any mediators and rearrange the nonphenolic β-O-4 lignin model compound in the presence of mediators, which provide *in vivo* validation for their lignin degradation activity. However, APPL production was not completely eliminated by the laccase deficient strain, so other yet to be discovered enzymes likely are also involved in lignin degradation.

ASSOCIATED CONTENT

Supporting Information

Primers used in this study (Table S1), structural motif of lignin (Figure S1), lignin model compounds (Figure S2), dependence of steady-state kinetic parameters of SCLAC on pH (Figure S3), multiple-sequence alignment of small laccases (Figure S4), coordination geometry of the H_2O_2 intermediate bound to the trinuclear center copper atoms and water molecules in AMLAC (Figure S5), zinc metal ion binding site of SVLAC (Figure S6), ESI-MS showing the formation of the ketone derivative (Figure S7), SDS–PAGE of purified small laccases (Figure S8), ESI-MS showing the formation of oxidative products (Figure S9), and proposed oxidative mechanism of the lignin model compound (Scheme S1). This material is available free of charge via the Internet at http://pubs.acs.org.

Accession Codes

PDB entries 3TA4 (AMLAC·Cu^{2+}·LM-OMe), 3T9W (AMLAC·Cu^{2+}), 3TBB (SVLAC·Cu^{2+}·Zn^{2+}), 3TAS (SVLAC·Cu^{2+}), and 3TBC (SVLAC·Cu^{2+}·AV).

AUTHOR INFORMATION

Corresponding Author

*Department of Chemical Engineering, Columbia University, New York, NY 10027. E-mail: sm3577@columbia.edu. Telephone: (212) 854-1444.

Present Addresses

§S.M.: Department of Chemical Engineering, Columbia University, New York, NY 10027.

∥T.L.: Cornell University, Ithaca, NY 14853.

Funding

This research was supported by the Energy Biosciences Institute, University of Illinois at Urbana-Champaign. Use of the Advanced Photon Source was supported by the U.S. Department of Energy, Office of Sciences, under Contact DE-AC02-06CH11357. LS-CAT Sector 21 is supported by the Michigan Economic Development Corp. and the Michigan Technology Tri-Corridor (Grant 085P1000817).

Notes

The authors declare no competing financial interest.

ABBREVIATIONS

LiP, lignin peroxidase; MnP, manganese peroxidase; SCLAC, *S. coelicolor* laccase; SLLAC, *S. lividans* laccase; SVLAC, *S. viridosporus* laccase; AMLAC, *Amycolatopsis* laccase; TAT, twin-arginine translocation; LM-OMe, 1-(3,4-dimethoxyphenyl)-2-(2-methoxyphenoxy)-1,3-dihydroxypropane; LM-OH, 1-(3-methoxy-4-hydroxy)-2-(2-methoxyphenoxy)-1,3-dihydroxypropane; ABTS, 2,2′-azinobis(3-ethylbenzothiazoline-6-sulfonate); DMP, 2,6-dimethoxyphenol; AV, acetovanillone; HOBt, hydroxybenzotriazole; CH_3CN, acetonitrile; DMSO, dimethyl sulfoxide; $MgCl_2$, magnesium chloride; NaCl, sodium chloride; HCl, hydrochloric acid; KCl, potassium chloride; Na_2HPO_4, disodium hydrogen phosphate; KH_2PO_4, potassium dihydrogen phosphate; $CuSO_4$, copper sulfate; DMF, dimethylformamide; PBS, phosphate-buffered saline; dNTP, deoxyribonucleotide; FAD, flavin adenine dinucleotide; LB, Luria-Bertani; IPTG, isopropyl β-D-1-thiogalactopyranoside; 3-HAA, 3-hydroxyanthranilic acid; OD, optical density; HPLC, high-performance liquid chromatography; LC–MS-IT-TOF, liquid chromatography and mass spectrometry ion trap time-of-flight; PCR, polymerase chain reaction; UV–vis, ultraviolet–visible; k_{rel}, relative rate constant; K_{app}, apparent K_M.

REFERENCES

(1) Adler, E. (1977) Lignin chemistry: Past, present and future. *Wood Sci. Technol. 11*, 169–218.

(2) El Hage, R., Chrusciel, L., Desharnais, L., and Brosse, N. (2010) Effect of autohydrolysis of *Miscanthus x giganteus* on lignin structure and organosolv delignification. *Bioresour. Technol. 101*, 9321−9329.
(3) Villaverde, J. J., Li, J., Ek, M., Ligero, P., and de Vega, A. (2009) Native lignin structure of *Miscanthus x giganteus* and its changes during acetic and formic acid fractionation. *J. Agric. Food Chem. 57*, 6262−6270.
(4) Klinke, H. B., Thomsen, A. B., and Ahring, B. K. (2004) Inhibition of ethanol-producing yeast and bacteria by degradation products produced during pre-treatment of biomass. *Appl. Microbiol. Biotechnol. 66*, 10−26.
(5) Palmqvist, E., and Hahn-Hagerdal, B. (2000) Fermentation of lignocellulosic hydrolysates. I: Inhibition and detoxification. *Bioresour. Technol. 74*, 17−24.
(6) Palmqvist, E., and Hahn-Hagerdal, B. (2000) Fermentation of lignocellulosic hydrolysates. II: Inhibitors and mechanisms of inhibition. *Bioresour. Technol. 74*, 25−33.
(7) Ander, P., and Eriksson, K. E. (1978) Lignin degradation and utilization by microorganisms. *Prog. Ind. Microbiol. 14*, 1−58.
(8) Kirk, T. K., and Farrell, R. L. (1987) Enzymatic "combustion": The microbial degradation of lignin. *Annu. Rev. Microbiol. 41*, 465−505.
(9) Moyson, E., and Verachtert, H. (1993) Microbial degradation of lignin. *Microb. Biotechnol. 58*, 1651−1653.
(10) Abdel-Hamid, A. M., Solbiati, J. O., and Cann, I. K. (2013) Insights into lignin degradation and its potential industrial applications. *Adv. Appl. Microbiol. 82*, 1−28.
(11) Kirk, T. K. (1981) Principles of lignin degradation by white-rot fungi. *Ekman-Days 1981, Int. Symp. Wood Pulping Chem. 3*, 66−70.
(12) Tuor, U., Winterhalter, K., and Fiechter, A. (1995) Enzymes of white-rot fungi involved in lignin degradation and ecological determinants for wood decay. *J. Biotechnol. 41*, 1−17.
(13) Iyer, A. P., and Mahadevan, A. (2002) Lignin degradation by bacteria. *Prog. Ind. Microbiol. 36*, 311−330.
(14) Brown, M. E., Walker, M. C., Nakashige, T. G., Iavarone, A. T., and Chang, M. C. (2011) Discovery and characterization of heme enzymes from unsequenced bacteria: Application to microbial lignin degradation. *J. Am. Chem. Soc. 133*, 18006−18009.
(15) Bugg, T. D., Ahmad, M., Hardiman, E. M., and Singh, R. (2011) The emerging role for bacteria in lignin degradation and bio-product formation. *Curr. Opin. Biotechnol. 22*, 394−400.
(16) Kirby, R. (2006) Actinomycetes and lignin degradation. *Adv. Appl. Microbiol. 58*, 125−168.
(17) Crawford, D. L. (1986) The role of actinomycetes in the decomposition of lignocellulose. *Symp. Biol. Hung. 32*, 715−728.
(18) Ramachandra, M., Crawford, D. L., and Hertel, G. (1988) Characterization of an extracellular lignin peroxidase of the lignocellulolytic actinomycete *Streptomyces viridosporus*. *Appl. Environ. Microbiol. 54*, 3057−3063.
(19) Thomas, L., and Crawford, D. L. (1998) Cloning of clustered *Streptomyces viridosporus* T7A lignocellulose catabolism genes encoding peroxidase and endoglucanase and their extracellular expression in *Pichia pastoris*. *Can. J. Microbiol. 44*, 364−372.
(20) Wang, Z., Bleakley, B. H., Crawford, D. L., Hertel, G., and Rafii, F. (1990) Cloning and expression of a lignin peroxidase gene from *Streptomyces viridosporus* in *Streptomyces lividans*. *J. Biotechnol. 13*, 131−144.
(21) Godden, B., Ball, A. S., Helvenstein, P., McCarthy, A. J., and Penninckx, M. J. (1992) Towards elucidation of the lignin degradation pathway in actinomycetes. *J. Gen. Microbiol. 138*, 2441−2448.
(22) Ramachandra, M., Crawford, D. L., and Pometto, A. L. (1987) Extracellular Enzyme Activities during Lignocellulose Degradation by *Streptomyces* spp.: A Comparative Study of Wild-Type and Genetically Manipulated Strains. *Appl. Environ. Microbiol. 53*, 2754−2760.
(23) Brown, M. E., Barros, T., and Chang, M. C. (2012) Identification and characterization of a multifunctional dye peroxidase from a lignin-reactive bacterium. *ACS Chem. Biol. 7*, 2074−2081.
(24) Machczynski, M. C., Vijgenboom, E., Samyn, B., and Canters, G. W. (2004) Characterization of SLAC: A small laccase from *Streptomyces coelicolor* with unprecedented activity. *Protein Sci. 13*, 2388−2397.
(25) Gianfreda, L., Xu, F., and Bollag, J.-M. (1999) Laccases: A useful group of oxidoreductive enzymes. *Biochem. J. 3*, 1−25.
(26) Mayer, A. M., and Staples, R. C. (2002) Laccase: New functions for an old enzyme. *Phytochemistry 60*, 551−565.
(27) Dwivedi, U. N., Singh, P., Pandey, V. P., and Kumar, A. (2011) Structure-function relationship among bacterial, fungal and plant laccases. *J. Mol. Catal. B: Enzym. 68*, 117−128.
(28) Ferrer, M., Beloqui, A., and Golyshin, P. N. (2010) Screening metagenomic libraries for laccase activities. *Methods Mol. Biol. (N.Y., NY, U.S.) 668*, 189−202.
(29) Youn, H.-D., Hah, Y. C., and Kang, S.-O. (1995) Role of laccase in lignin degradation by white-rot fungi. *FEMS Microbiol. Lett. 132*, 183−188.
(30) Eggert, C., Temp, U., and Eriksson, K.-E. L. (1997) Laccase is essential for lignin degradation by the white-rot fungus *Pycnoporus cinnabarinus*. *FEBS Lett. 407*, 89−92.
(31) Skalova, T., Dohnalek, J., Ostergaard, L. H., Ostergaard, P. R., Kolenko, P., Duskova, J., Stepankova, A., and Hasek, J. (2009) The Structure of the Small Laccase from *Streptomyces coelicolor* Reveals a Link between Laccases and Nitrite Reductases. *J. Mol. Biol. 385*, 1165−1178.
(32) Bauer, S., Sorek, H., Mitchell, V. D., Ibanez, A. B., and Wemmer, D. E. (2012) Characterization of *Miscanthus giganteus* lignin isolated by ethanol organosolv process under reflux condition. *J. Agric. Food Chem. 60*, 8203−8212.
(33) Kieser, T., Bibb, M. J., Buttner, M. J., Chater, K. F., and Hopwood, D. A. (2000) Practical Streptomyces Genetics. *Int. Microbiol. 3*, 260−261.
(34) Gust, B., Challis, G. L., Fowler, K., Kieser, T., and Chater, K. F. (2003) PCR-targeted *Streptomyces* gene replacement identifies a protein domain needed for biosynthesis of the sesquiterpene soil odor geosmin. *Proc. Natl. Acad. Sci. U.S.A. 100*, 1541−1546.
(35) Crawford, D. L., and Pometto, A. L., III (1988) Acid-precipitable polymeric lignin: Production and analysis. *Methods Enzymol. 161*, 35−47.
(36) Motulsky, H., and Christopoulos, A. (2004) *Fitting Models to Biological Data using Linear and Nonlinear Regression. A Practicle Guide to Curve Fitting*, Oxford University Press, New York.
(37) Kabsch, W. (2010) Integration, scaling, space-group assignment and post-refinement. *Acta Crystallogr. D66*, 133−144.
(38) Camarero, S., Ibarra, D., Martínez, Á. T., Romero, J., Gutiérrez, A., and del Río, J. C. (2007) Paper pulp delignification using laccase and natural mediators. *Enzyme Microb. Technol. 40*, 1264−1271.
(39) Diaz-Gonzalez, M., Vidal, T., and Tzanov, T. (2011) Phenolic compounds as enhancers in enzymatic and electrochemical oxidation of veratryl alcohol and lignins. *Appl. Microbiol. Biotechnol. 89*, 1693−1700.
(40) Vallee, B. L., and Auld, D. S. (1993) Zinc: Biological functions and coordination motifs. *Acc. Chem. Res. 26*, 543−551.
(41) McCoy, A. J., Grosse-Kunstleve, R. W., Adams, P. D., Winn, M. D., Storoni, L. C., and Read, R. J. (2007) Phaser crystallographic software. *J. Appl. Crystallogr. 40*, 658−674.
(42) Lamzin, V. S., and Wilson, K. S. (1997) Automated refinement for protein crystallography. *Methods Enzymol. 277*, 269−305.
(43) Emsley, P., Lohkamp, B., Scott, W. G., and Cowtan, K. (2010) Features and development of Coot. *Acta Crystallogr. D66*, 486−501.
(44) Adams, P. D., Afonine, P. V., Bunkoczi, G., Chen, V. B., Davis, I. W., Echols, N., Headd, J. J., Hung, L. W., Kapral, G. J., Grosse-Kunstleve, R. W., McCoy, A. J., Moriarty, N. W., Oeffner, R., Read, R. J., Richardson, D. C., Richardson, J. S., Terwilliger, T. C., and Zwart, P. H. (2010) PHENIX: A comprehensive Python-based system for macromolecular structure solution. *Acta Crystallogr. D66*, 213−221.
(45) Harwood, C. S., and Parales, R. E. (1996) The *β*-ketoadipate pathway and the biology of self-identity. *Annu. Rev. Microbiol. 50*, 553−590.
(46) Ahmad, M., Taylor, C. R., Pink, D., Burton, K., Eastwood, D., Bending, G. D., and Bugg, T. D. (2010) Development of novel assays

for lignin degradation: Comparative analysis of bacterial and fungal lignin degraders. *Mol. BioSyst. 6*, 815−821.
(47) Lahtinen, M., Kruus, K., Boer, H., Kemell, M., Andberg, M., Viikari, L., and Sipila, J. (2009) The effect of lignin model compound structure on the rate of oxidation catalyzed by two different fungal laccases. *J. Mol. Catal. B: Enzym. 57*, 204−210.
(48) Jeffries, T. W. (1990) Biodegradation of lignin-carbohydrate complexes. *Biodegradation 1*, 163−176.
(49) Arora, D. S., and Sharma, R. K. (2010) Ligninolytic fungal laccases and their biotechnological applications. *Appl. Biochem. Biotechnol. 160*, 1760−1788.
(50) Dube, E., Shareck, F., Hurtubise, Y., Beauregard, M., and Daneault, C. (2008) Decolorization of recalcitrant dyes with a laccase from *Streptomyces coelicolor* under alkaline conditions. *J. Ind. Microbiol. Biotechnol. 35*, 1123−1129.
(51) Leonowicz, A., Cho, N. S., Luterek, J., Wilkolazka, A., Wojtas-Wasilewska, M., Matuszewska, A., Hofrichter, M., Wesenberg, D., and Rogalski, J. (2001) Fungal laccase: Properties and activity on lignin. *J. Basic Microbiol. 41*, 185−227.
(52) Li, K., Xu, F., and Eriksson, K. E. (1999) Comparison of fungal laccases and redox mediators in oxidation of a nonphenolic lignin model compound. *Appl. Environ. Microbiol. 65*, 2654−2660.
(53) Andreu, G., and Vidal, T. (2011) Effects of laccase-natural mediator systems on kenaf pulp. *Bioresour. Technol. 102*, 5932−5937.
(54) Mitchell, V., Taylor, C., and Bauer, S. (2013) Comprehensive Analysis of Monomeric Phenolics in Dilute Acid Plant Hydrolysates. *BioEnergy Res.*, 1−16.
(55) Hammel, K. E., Jensen, K. A., Jr., Mozuch, M. D., Landucci, L. L., Tien, M., and Pease, E. A. (1993) Ligninolysis by a purified lignin peroxidase. *J. Biol. Chem. 268*, 12274−12281.
(56) Marzullo, L., Cannio, R., Giardina, P., Santini, M. T., and Sannia, G. (1995) Veratryl alcohol oxidase from *Pleurotus ostreatus* participates in lignin biodegradation and prevents polymerization of laccase-oxidized substrates. *J. Biol. Chem. 270*, 3823−3827.
(57) Lyashenko, A. V., Zhukova, Y. N., Zhukhlistova, N. E., Zaitsev, V. N., Stepanova, E. V., Kachalova, G. S., Koroleva, O. V., Voelter, W., Betzel, C., Tishkov, V. I., Bento, I., Gabdulkhakov, A. G., Morgunova, E. Y., Lindley, P. F., and Mikhailov, A. M. (2006) Three-dimensional structure of laccase from *Coriolus zonatus* at 2.6 Å resolution. *Crystallogr. Rep. 51*, 817−823.
(58) Polyakov, K. M., Fedorova, T. V., Stepanova, E. V., Cherkashin, E. A., Kurzeev, S. A., Strokopytov, B. V., Lamzin, V. S., and Koroleva, O. V. (2009) Structure of native laccase from *Trametes hirsuta* at 1.8 Å resolution. *Acta Crystallogr. D65*, 611−617.
(59) Ge, H., Gao, Y., Hong, Y., Zhang, M., Xiao, Y., Teng, M., and Niu, L. (2010) Structure of native laccase B from *Trametes sp.* AH28-2. *Acta Crystallogr. F66*, 254−258.
(60) Bonomo, R. P., Cennamo, G., Purrello, R., Santoro, A. M., and Zappala, R. (2001) Comparison of three fungal laccases from *Rigidoporus lignosus* and *Pleurotus ostreatus*: Correlation between conformation changes and catalytic activity. *J. Inorg. Biochem. 83*, 67−75.
(61) Enguita, F. J., Martins, L. O., Henriques, A. O., and Carrondo, M. A. (2003) Crystal structure of a bacterial endospore coat component. A laccase with enhanced thermostability properties. *J. Biol. Chem. 278*, 19416−19425.
(62) Bento, I., Martins, L. O., Gato Lopes, G., Armenia Carrondo, M., and Lindley, P. F. (2005) Dioxygen reduction by multi-copper oxidases; a structural perspective. *Dalton Trans.*, 3507−3513.
(63) Durao, P., Bento, I., Fernandes, A. T., Melo, E. P., Lindley, P. F., and Martins, L. O. (2006) Perturbations of the T1 copper site in the CotA laccase from *Bacillus subtilis*: Structural, biochemical, enzymatic and stability studies. *JBIC, J. Biol. Inorg. Chem. 11*, 514−526.
(64) Kallio, J. P., Auer, S., Janis, J., Andberg, M., Kruus, K., Rouvinen, J., Koivula, A., and Hakulinen, N. (2009) Structure-function studies of a *Melanocarpus albomyces* laccase suggest a pathway for oxidation of phenolic compounds. *J. Mol. Biol. 392*, 895−909.